

# LPHYS2162 Project - Feedback temperature dependence

Augustin Lambotte, Maxence Malempré  
Université catholique de Louvain, École de Physique,  
Chemin de Cyclotron 2, 1348 Louvain-la-Neuve, Belgique\*

During the last two centuries humanity has released greenhouse gases in the atmosphere,  $CO_2$  for the main part. Due to the thermal infrared absorption, an increase in the concentration of these gases induces an increase in forcing which leads to planet warming. Evaluate the earth sensitivity, i.e. the rise in global temperature following a doubling of  $CO_2$  concentration from the pre-industrial level, is crucial in the global warming context we are facing in the 21th century. In this paper we will use a zero dimensional energy model to investigate the warming response to a given forcing taking into account the possible feedback temperature dependence. We will test some parameter values for these - drawn for physical arguments and GCM's - and see how they affect the long term warming. We will study how positive feedback temperature dependence tends to increase earth sensitivity and doing so, produce more warming, and inversely for negative one.

## INTRODUCTION

In this paper we will investigate how feedback temperature dependence affect the climate sensitivity. It is often assumed that the warming caused by an increase in  $CO_2$  concentration is proportional to the forcing  $F$  caused by this perturbation  $\Delta T = -F/\lambda$  with  $\lambda$  a constant. So that the temperature feedback on the forcing is linear,  $-F = \lambda\Delta T$ . This relation is acceptable for small  $CO_2$  increases and this is why we call it *pre-industrial* feedback. It is the feedback that we could expect for a small change in  $CO_2$  concentration from the pre-industrial values.

For larger forcing, however, this linear approximation doesn't seem correct[5]. As the earth's temperature rises, some of its characteristics change, leading to a modification of its sensitivity. For example, if a state warm enough is reached, the ice coverage on earth will decrease significantly and as it does, the planet will warm even more under a given forcing. This is an example of positive feedback temperature dependence. An example of negative temperature dependence feedback can be found in [2]. A temperature rise leads to a more cloudy sky with an higher albedo, lowering the climate sensitivity. Taking account of these effects is crucial if we don't want to underestimate the long time effect of greenhouse gases emissions. Note that there is also a feedback  $CO_2$  dependence but its effects on  $\Delta T$  are smaller than the feedback temperature dependence, we will ignore it in this paper.

We add a quadratic dependence in temperature to take into account this feedback temperature dependence and we analyse this system in Part I. Particular emphasis will be placed on the cases where the linear model breaks down. We compare the behaviour of the model under one and two doubling of  $CO_2$  concentration and we perform several simulations with different values of parameter. A runaway warming will be observed for some cases leading, in the long run, to an infinite warming which is not physical.

In the second part of this paper we will add a fifth order dependence term in temperature to our model to

avoid these unphysical runaways warming observed in Part I and see what happens now in these cases. We will study the equilibrium points of our new system and their stability which will display a tipping point. Finally we will see how the system behaves if we add a Gaussian noise to simulate the chaotic fluctuations of the climate system. This will highlight how the presence of tipping point make difficult the prediction of system behaviour.

All the code used for the following simulations and all the relevant plots and animations can be found on the GitHub <https://github.com/AugustinLambotte/LPHYS2162.Project.git>.

## PART I

### Model description

Let  $N$  be the net, top-of-atmosphere energy flux. We suppose that we have a steady state for pre-industrial conditions given by  $T_0 \approx 287K$  and  $CO_{20} \approx 270ppm$ , i.e  $N(T_0, CO_{20}) = 0$ . If we have a perturbation in the  $CO_2$  concentration we are going to observe a change in  $N$  represented by  $F$ , the forcing. For a given multiplication by  $n$  of the atmospheric  $CO_2$  concentration, the forcing is given by  $F_{n\times} = 3.71 \log_2(n) Wm^{-2}$ . If  $F > 0$  the earth temperature will increase and also modify the forcing following,

$$-F = \lambda\Delta T + \alpha\Delta T^2. \quad (1)$$

until we reach a new steady state (if it's possible).  $\lambda$  is called the *pre-industrial* feedback, it is the slope of  $N$  at  $T_0$ . A negative  $\lambda$  implies a stable pre-industrial earth.  $\alpha$  is the feedback temperature dependence. Estimation of its value is hard to achieve but an attempt can be made in light of GCM and physical discussion. From GCM's [1] has found  $-0.04 < \alpha < 0.06 Wm^{-2} K^{-2}$ . We can compute the feedback temperature dependence for some well known effects : for example we know the Planck effect where the

earth irradiates energy following  $\sigma T^4$ . So the feedback temperature dependence associated  $\alpha_{planck}$  would be

$$\alpha_{planck} = \frac{1}{2} \frac{d^2(\sigma T^4)}{dT^2} \Big|_{255K} \approx -0.02 W m^{-2} K^{-2} \quad (2)$$

The Planck feedback becomes more negative under warming. Indeed, negative  $\alpha$  implies that the feedback becomes more negative during the warming and so the equilibrium temperature will be lower with the feedback temperature dependence. In the other way a positive  $\alpha$  will make the feedback less negative during the warming and a steady state will be met at a highest temperature than for a linear feedback alone.

Given a forcing  $F_{n\times}$  due to a multiplication by  $n$  of the  $CO_2$  concentration, the steady state temperature increase is given by,

$$\Delta T_{n\times} = \frac{-\lambda - \sqrt{\lambda^2 - 4\alpha F_{n\times}}}{2\alpha} \quad (3)$$

if we assume quadratic dependence as in eq. 1. For a linear feedback -  $\alpha = 0$  - we will simply have  $\Delta T_{n\times} = -F_{n\times}/\lambda$ , as we said the linear approximation leads to a warming directly proportional to the forcing. It is important to note that eq. 3 has a real solution only if  $\lambda^2 > -4\alpha F_{n\times}$ . If the system parameters don't respect this inequality, the feedback will become positive before reaching the stability point and a runaway warming will appear. A temperature rise will lead to a forcing rise which will in return increase temperature. The forcing  $F_{n\times}$  and the pre-industrial feedback are the best known parameters of the system, so we will define a critical value  $\alpha_c$  as the maximum value that  $\alpha$  could take before a runaway warming happens.

$$\alpha_c = \frac{\lambda^2}{4F_{n\times}} \quad (4)$$

### Simulation

Now let's simulate eq. 1 to investigate its behaviour under different forcing and parameters values. We have plotted on fig. 1 different scenarios. Firstly we note that for  $\Delta T < 2K$  the quadratic and linear model have the same behaviour, it's only for stronger warming that we can observe a significant difference. On the above plot we see that the case with  $\alpha = 0.058 W m^{-2} K^{-2}$  leads to a runaway warming after one doubling of  $CO_2$  but in the second plot the same  $\alpha$  value curve needs two doubling of  $CO_2$  to present a runaway warming. As we could expect, bigger is the pre-industrial feedback magnitude, easier it is to reach a steady state.

As we said, we see on fig. 1 that the linear approximation holds valid for a certain range of temperature. To highlight how the linear approximation gives a valid

warming prediction under a given forcing, a more relevant question would be : on which forcing range the linear approximation remains valid ? We plot on fig. 2 six scenarios. Two pre-industrial feedbacks were set, on which we tested two different values of  $\alpha$ , and their linear approximations. The more negative the pre-industrial feedback, the more valid the linear approximation, and conversely. A bigger  $\alpha$  lessen the approximation acceptability. Eventually, for a given value of the parameters  $\lambda$  and  $\alpha$  the linear approximation accuracy decreases when the forcing increases.

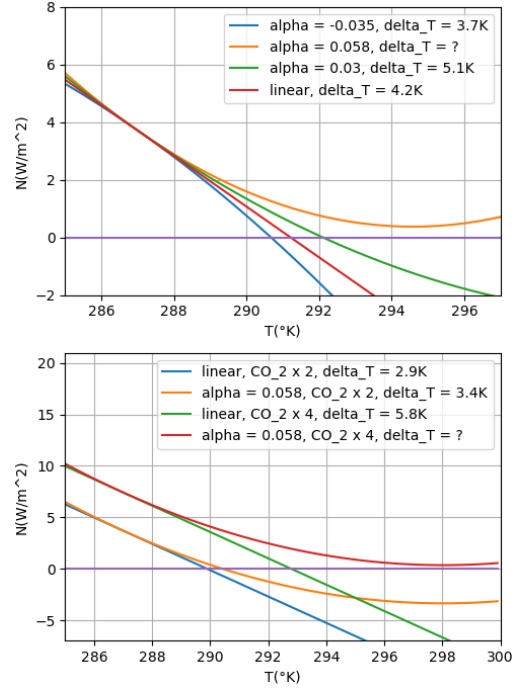


FIGURE 1 – Global annual mean net top-of-atmosphere energy flux  $N$  (downward positive) as a function of global annual mean surface temperature  $T$ , where each curve has a fixed  $CO_2$  concentration. **above :** doubling of  $CO_2$  concentration cause a forcing  $F_{2\times} = 3.71 W/m^2$ . All curves have the same pre-industrial feedback  $\lambda = -0.88 W m^{-2} K^{-1}$  and we test different values of  $\alpha$ . For  $\alpha = 0.058 W m^{-2} K^{-2}$  the feedback becomes positive near  $295^\circ K$  causing a runaway warming. **below :** All the curves have the same pre-industrial feedback  $\lambda = -1.28 W m^{-2} K^{-1}$ . Comparison between linear and quadratic model ( $\alpha = 0.058 W m^{-2} K^{-2}$ ) and between one and two doubling of  $CO_2$  concentration.

We have plotted on fig. 3 the temperature increase after one (above) and two (below) doubling of  $CO_2$  concentration in function of the feedback temperature parameter  $\alpha$ , each time for three different values of the pre-industrial feedback parameter  $\lambda$ . If  $\alpha = 0$  we are in the linear model and  $\Delta T_{4\times} = 2 \times \Delta T_{2\times}$ , for negative value of  $\alpha$  we have now that  $\Delta T_{4\times} < 2 \times \Delta T_{2\times}$  and finally we have

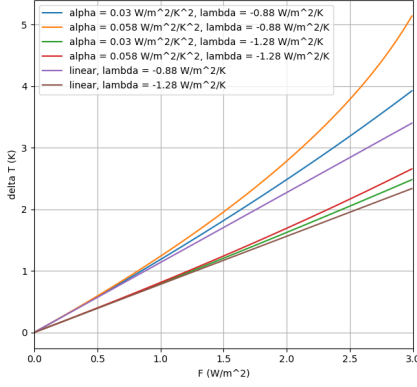


FIGURE 2 – Plotting of the expected warming value  $\Delta T$  in function of forcing for six scenarios. Two  $\lambda$  values are tested,  $\lambda = -1.28 \text{ W m}^{-2} \text{ K}^{-1}$  (the 3 lower curves) and  $\lambda = -0.88 \text{ W m}^{-2} \text{ K}^{-1}$  (the 3 upper curves). For each  $\lambda$  value we simulate 3 scenarios; a linear one, one with  $\alpha = 0.3 \text{ W m}^{-2} \text{ K}^{-2}$  and one with  $\alpha = 0.058 \text{ W m}^{-2} \text{ K}^{-2}$ . For the lowest  $\lambda$  value we see that the linear case is correct in first approximation in the range of forcing tested. For the biggest  $\lambda$  value the models predictions are diverging quickly from each other after  $F \approx 1 \text{ W/m}^2$ .

$\Delta T_{4\times} > 2 \times \Delta T_{2\times}$  for positive value of  $\alpha$ . As we said earlier, a bigger value of  $\alpha$  tends to increase the earth sensitivity when temperature rises. To highlight this behaviour we have plotted on a single graph  $\Delta T_{4\times}$  and  $2 \times \Delta T_{2\times}$  for a range of  $\alpha$  value and  $\lambda = -0.79 \text{ W m}^{-2} \text{ K}^{-1}$  on fig. 4. The two curves intersect each other for the linear approximation. Indeed the climate sensitivity is constant in this case because  $\Delta T_{n\times}$  is directly proportional to  $F_{n\times}$  and  $F_{2n\times} = 2 \times F_n$ . Finally we note, for positive value of  $\alpha$ , that the climate sensitivity increases at high rate. This shows how important it is to know the feedback temperature dependence for high warming prediction.

### Thermal inertia and transient behaviour of the model

We now consider the time evolution of the temperature increase  $\Delta T$ ,

$$C \frac{d\Delta T}{dt} = F + \lambda \Delta T + \alpha \Delta T^2 \quad (5)$$

With  $C = 8.36 \times 10^8 \text{ J K}^{-1} \text{ m}^{-2}$  the thermal inertia. We want to see the transient behaviour between the moment of the forcing and the moment where steady state is reached. We integrate numerically eq. 5 with a simple forward Euler method for the same parameters as in fig. 1 and we plot the results on fig. 5. We also made an animation of the transient behaviour with the same parameters as in fig. 3 varying with alpha on the Gi-

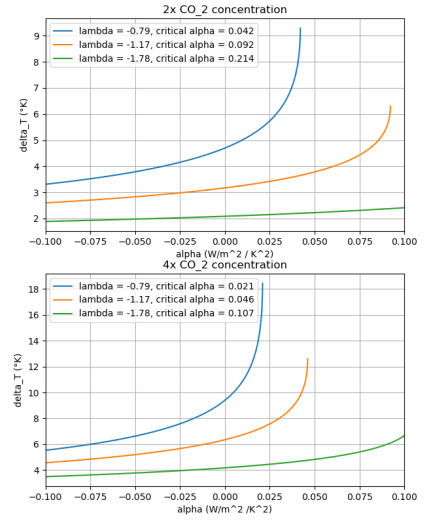


FIGURE 3 – Temperature increase in function of  $\alpha$  for three different pre-industrial feedbacks. **above** :After a doubling of  $\text{CO}_2$  concentration. **below** :After two doubling of  $\text{CO}_2$  concentration.

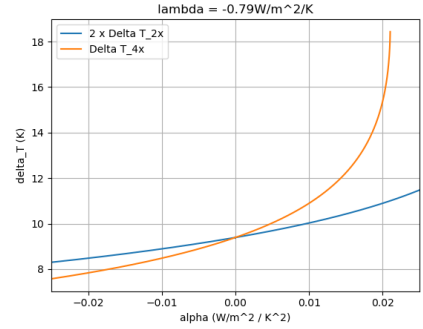


FIGURE 4 – Comparison between  $\Delta T_{4\times}$  and  $2 \times \Delta T_{2\times}$  for  $\lambda = -0.79 \text{ W m}^{-2} \text{ K}^{-1}$ . We see that for the linear model - i.e.  $\alpha = 0$  - the two curves intersect. Note how fast the  $\Delta T_{4\times}$  increase compare to  $2 \times \Delta T_{2\times}$  when  $\alpha$  become positive.

tHub at Animation/alpha\_dyn.co2x2.mp4 and Animation/alpha\_dyn.co2x4.mp4. We have the same steady state temperature and the same scenarios facing a runaway warming. As we could expect, the time that a simulation takes to reach a steady state increases with  $\alpha$ . We have plotted how the time taken to reach a steady state varies with alpha on fig. 6. As we could expect, the system takes longer time to stabilize at high  $\alpha$  value because the climate sensitivity increases during warming.

We note that for a given augmentation of  $\text{CO}_2$  concentration the different simulations have approximately the same behaviour for the first 25 years. After this "common path" the simulations with the biggest  $\alpha$  value take a longer time to reach the steady state and this steady state

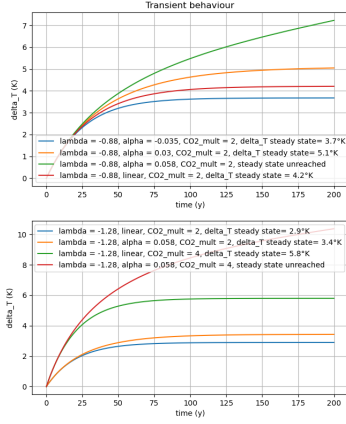


FIGURE 5 – *Temperature evolution in time under an augmentation of CO<sub>2</sub> concentration, all curves have the same parameters that the ones in fig. 1. We see that the steady states are reached at the same temperature value as in fig. 1. It is interesting to note that the simulations with a negative value of  $\alpha$  are reaching steady state faster than the ones with only a pre-industrial feedback which are also faster than the ones with a positive value of  $\alpha$ .*

is higher. This "common path" is interesting because it tells us that after a given forcing, it takes few decades before we can evaluate from data the magnitude of the temperature dependence feedback. This behaviour should encourage us to be careful with the anthropogenic forcing we apply on climate system. If the temperature dependence feedback is high this forcing could run to a runaway warming. But we couldn't know this before some decades and it would be too late to react.

### The runaway warming cases

A planetary runaway warming leading to infinity temperature, like the quadratic runaway we had before, is physically impossible.

Nevertheless some cases of runaway warming induced by large perturbations that lead the planet to a significantly warmer state is conceivable even if our quadratic model can't reach them. We can find in [4] an extended discussion about how the earth sensitivity could increase when temperature rises and the potential high warming which could occur. They explained that '*The warmer the climate becomes, the more it has to warm in order to balance a further CO<sub>2</sub> doubling because warming becomes less effective at rebalancing the flow of energy.*'. We can avoid this infinite quadratic runaway warming and find a new steady state by adding higher order terms in 1. We will see this in the next Part of the paper. As we are going

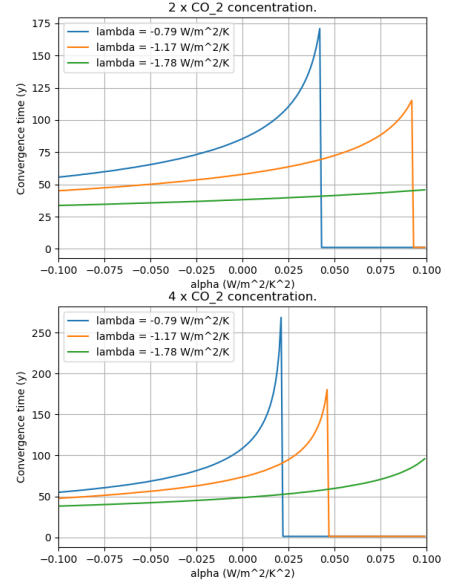


FIGURE 6 – *The time the system takes to reach a steady state with the same parameters values as in fig. 3. We note that the convergence time increase with  $\alpha$ . The point where the curve falls to 0 are the runaway point where any steady state can be reached.*

to observe, the quadratic runaway cases will lead to new steady state far away from the equilibrium we found until now.

## PART II

### Potential function

For further development we want to investigate the stability of our systems. We introduce here the *potential function* which will be useful to do so. Designated as  $V(T)$ , it is defined as follow,

$$\frac{dT}{dt} = -\frac{dV}{dT} \quad (6)$$

An equilibrium point  $T_0$  of our system is given by

$$\left. \frac{dT}{dt} \right|_{T_0} = 0 \Rightarrow \left. \frac{dV}{dT} \right|_{T_0} = 0 \quad (7)$$

So the position of the local maximum and minimum of  $V(T)$  give us the equilibrium point of our system. The shape of  $V(T)$  near  $T_0$  indicate the stability of our equilibrium. Reminding that  $N(T)$  is the net energy flux at the top of the atmosphere we have,

$$\frac{dT}{dt} = N(T) \quad \text{and} \quad N(T_0) = 0 \quad (8)$$

If we consider a little perturbation  $T'(t)$  around  $T_0$ , we have that

$$\frac{d(T_0 + T'(t))}{dt} = N(T_0 + T'(t)) \approx N(T_0) + \left. \frac{dN}{dT} \right|_{T_0} T'(t) \quad (9)$$

So the time evolution of our perturbation follows,

$$\frac{dT'}{dt} = \left. \frac{dN}{dT} \right|_{T_0} T'(t) = -\gamma T'(t) \quad , \quad \gamma = -\left. \frac{d^2V}{dT^2} \right|_{T_0} \quad (10)$$

$$\Rightarrow T'(t) = T'(0)e^{-\gamma t} \quad (11)$$

Hence, a stable point is characterized by a positive value of the second derivative of the potential function at this point.

### Correction of unphysical runaway warming

As we have seen the quadratic feedback model eq. 1 presents a runaway warming behaviour if the forcing is too high, leading to an infinite planet's temperature. To avoid this unphysical behaviour we will add in eq. 1 a higher order term in  $\Delta T$ .

$$C \frac{d\Delta T}{dt} = F + \lambda \Delta T + \alpha \Delta T^2 + \beta \Delta T^5 \quad (12)$$

A negative value of  $\beta$  will lead to a negative feedback at high temperature, which will overbalance a quadratic runaway warming. We will now make use of the potential function we have defined earlier. In our case  $V(T)$  is given by,

$$V(T) = -\frac{1}{C} \int_0^T [F + \lambda \Delta T' + \alpha \Delta T'^2 + \beta \Delta T'^5] dT' \quad (13)$$

We can see on fig. 7 a comparison between the potential function of our new system given by eq. 12 and the first we have studied - eq. 5 - for different forcing values. In this presentation with potential function we find the equilibrium point at the local extremum as we said. For example in the first scenario with no forcing we see that the initial condition - i.e.  $T_0 = 287K$  - is at the minimum of the potential function and is therefore at an equilibrium point. Furthermore this equilibrium is stable for the two cases (quadratic and fifth order term), we see that after a little perturbation the system will go back to the equilibrium point, following the slope of  $V(T)$ . We can find unstable equilibrium at the local maximum of  $V(T)$ . Let's take, for example, the fourth scenario of the fifth order equation system. It has two minimum and one maximum in the range  $T \in [282, 307]$ , so with the initial condition  $T_0 = 287K$  it reaches the stable equilibrium  $T = 293.4K$ . But if, for some reason, the system was to be pushed to the local maximum it would be in an unstable equilibrium and a tiny perturbation would push it in one of the two stable equilibrium around him.

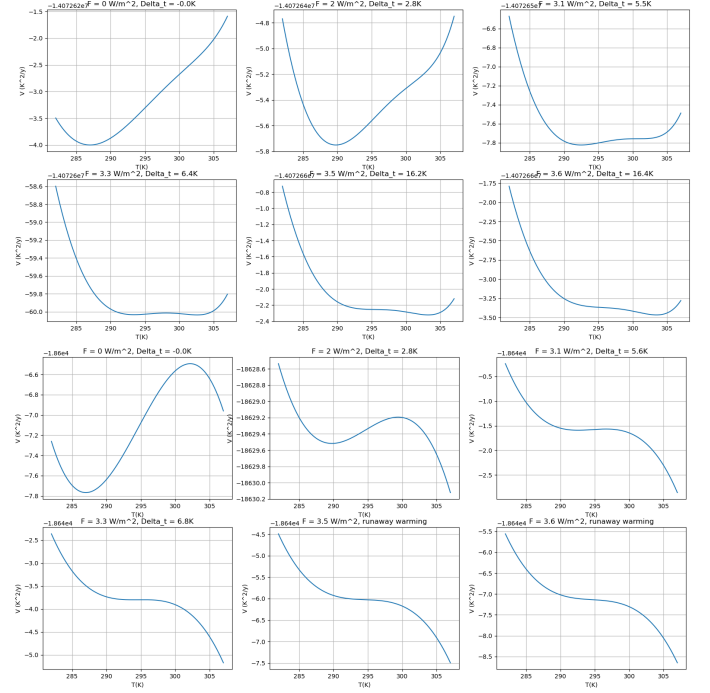


FIGURE 7 – Potential function plots for successively rising forcings.  $\alpha = 0.058 Wm^{-2}K^{-2}$  and  $\lambda = -0.88 Wm^{-2}K^{-1}$  are the same parameters values for every simulations. The six above are with a five order term corresponding to the coefficient  $\beta = -4 \times 10^{-6} Wm^{-2}K^{-5}$  as in eq. 13 and the six below don't have a 5 order dependence, i.e  $\beta = 0$  in eq. 13. We see that the negative value of  $\beta$  stabilizes the system at a closer temperature compared to the quadratic system and avoids the runaway warming that occurs for the  $F = 3.5 Wm^{-2}$  and  $F = 3.6 Wm^{-2}$  cases. An animated video of the fifth order potential varying with the forcing value can be found on the GitHub at [Animation/Potential\\_variation\\_with\\_time.mp4](#)

We note that, until the fourth scenario, the temperature increase of the quadratic system and order 5 system are comparable. For these forcing values the quadratic runaway doesn't happen yet and the system stabilizes at the "quadratic equilibrium point". It's only in scenario 5 and 6 that the quadratic runaway appears and make disappear the first equilibrium point. While the quadratic system just runaway, the fifth order one finds an other equilibrium point further. This is what we wanted, a runaway warming is now possible for high forcing without becoming unphysical.

### Transient behaviour

Now that we have seen the behaviour we could expect from our system we will integrate eq. 12 in time and link



interesting patterns from fig. 7 to the transient behaviour. First we will plot the time evolution with two different forcing values,  $F = 3.45 \text{ W/m}^2$  and  $F = 3.5 \text{ W/m}^2$ . They are chosen to be just before and just after the critical  $F$  value where the quadratic model runs away. We see on fig. 8 their time evolution. The first one reaches a steady state that could be qualified of "quadratic steady state". In the second scenario with  $F = 3.5 \text{ W/m}^2$  the system presents a quadratic runaway and find the "fifth order equilibrium" at a warming point approximately twice bigger.

We plotted in fig. 9 the temperature increase and the convergence time associated with the given forcing. It highlights what we have seen, for a given forcing around  $F = 3.5 \text{ W/m}^2$  the stability isn't reached anymore at  $\Delta T \approx 8 \text{ K}$  and the planet has to warm until a new equilibrium is hit, around  $\Delta T \approx 16 \text{ K}$ . The convergence time peaking at this transition is the reflect of the gentle slope between  $\Delta T \approx 8 \text{ K}$  and  $\Delta T \approx 16 \text{ K}$  that we can observe in the last scenarios of fig. 7. The point located at  $\Delta T = 8 \text{ K}$  isn't in equilibrium anymore, it now moves to the new steady state very slowly because the slope is low. A dynamical evolution of the changing equilibrium point can be found on the github at [Animation/Time\\_evolution\\_order5\\_model.mp4](#).

As we see in fig. 8, the eq. 12 leads to a situation where at some point, the temperature increase doubles under a little rise in forcing. This is a tipping point situation, where a little perturbation produce a large change in planet's characteristic. There is several important possible tipping points in the earth system and understand such behaviours is crucial to avoid important climate perturbations [7] [6].

### Gaussian noise

Until now our system was totally deterministic but we want to study how the chaotic fluctuations of the climate system affect the dynamics of our model. The simplest way to do that is to add a Gaussian white noise term in eq. 12. We are now dealing with the following system,

$$C \frac{d\Delta T}{dt} = F + \lambda \Delta T + \alpha \Delta T^2 + \beta \Delta T^5 + D\xi(t) \quad (14)$$

with  $\xi(t)$  our Gaussian white noise,  $\mathbb{E}[\zeta(t), \zeta(s)] = \delta_{ts}$ . The amplitude of the noise is set at  $D = 5753 \text{ Wm}^{-2} \text{ s}^{1/2}$ . This make the standard deviation of the temperature fluctuation at the stationary state with no forcing is about  $0.15 \text{ K}$  - which is in accordance with annual global temperature fluctuations. Let's see how this new term impacts the system evolution. The figures fig. 10, 11 and 12 show the time evolution and pdf of a wide range of stochastic evolutions, their mean and the deterministic behaviour - i.e. with  $D = 0$ . We observe that the global shape of the stochastic evolution behaves like the deterministic one

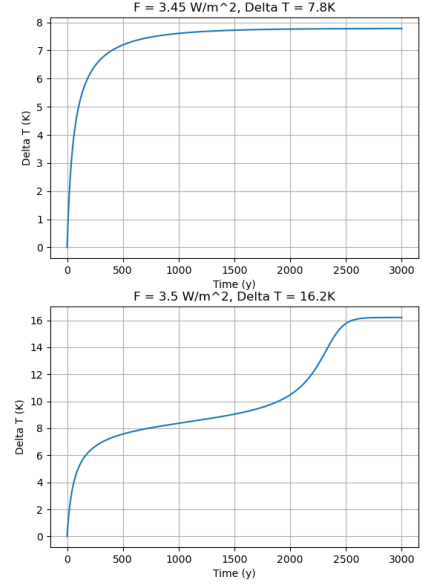


FIGURE 8 – Transient behaviour as described by eq. 12 with  $\lambda = -0.88 \text{ Wm}^{-2} \text{ K}^{-1}$ ,  $\alpha = 0.058 \text{ Wm}^{-2} \text{ K}^{-2}$  and  $\beta = -4 \times 10^{-8} \text{ Wm}^{-2} \text{ K}^{-5}$ . The simulations have been run with two near forcing values,  $F = 3.45 \text{ Wm}^{-2}$  above and  $F = 3.5 \text{ Wm}^{-2}$  below. However we note a totally different behaviour, whereas the first one finds a steady state at  $\Delta T = 7.8 \text{ K}$  the second stabilizes at  $\Delta T = 16.2 \text{ K}$ , a bit more than twice the first value. The system has a tipping point between these two forcing values.

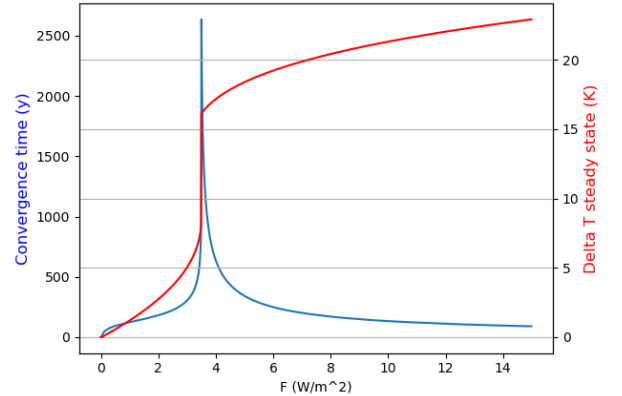


FIGURE 9 – We plotted the the steady state temperature increase,  $\Delta T$ , and the convergence time of our model for the system described by eq. 12 to highlight the tipping point behaviour. The simulation has been run with  $\alpha = 0.058 \text{ Wm}^{-2} \text{ K}^{-2}$ ,  $\lambda = -0.88 \text{ Wm}^{-2} \text{ K}^{-1}$  and  $\beta = -4 \times 10^{-8} \text{ Wm}^{-2} \text{ K}^{-5}$ . There is an abrupt doubling of the steady state  $\Delta T$  around  $F = 3.5 \text{ Wm}^{-2}$ .

and the mean value, if evaluated over enough simulation, corresponds to the deterministic value.

We see that the standard deviation isn't constant relative to the forcing, we plotted on fig. 13 an evolution of the standard deviation of the steady state with respect to the forcing, before and after the tipping point. We observe that the standard deviation tends to increase with  $F$  before the tipping point, passing from its unperturbed system value of  $0.15K$  to almost the double at  $F = 3Wm^{-2}$ . We didn't compute the standard deviation for  $F \in [3, 4]$  around the tipping, we discuss this behaviour in the next subsection. For  $F > 4Wm^{-2}$  however, we have an inverse behaviour and the standard deviation of the simulation set decreases while the forcing increases.

This behaviour is understandable in light of the potential function curve. Indeed as we show in eq. 11, the time the system takes to come back to the equilibrium point is relative to the second derivative of the potential function at the equilibrium point. We plotted the value of  $\partial^2 V / \partial T^2$  at the equilibrium point on fig. 14. This behaviour relies on what we observed on fig. 13, before the tipping point the standard deviation increases with  $F$  as  $\partial^2 V / \partial T^2$  decreases. The system takes more time to "catch up" a perturbation and doing so they are free to spread on a wider range. After the tipping point,  $\partial^2 V / \partial T^2$  increases with  $F$  and so the standard deviation decreases, the perturbations are "caught up" faster.

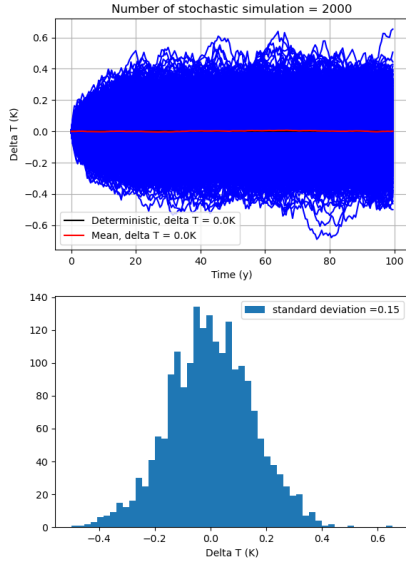


FIGURE 10 – Evolution of 2000 simulations following the stochastic equation eq. 14 with  $\lambda = -0.88Wm^{-2}K^{-1}$ ,  $\alpha = 0.058Wm^{-2}K^{-2}$  and  $\beta = -4 \times 10^{-8}Wm^{-2}K^{-5}$ . No forcing has been applied. We see, as expected, that the standard deviation is about  $0.15K$ .

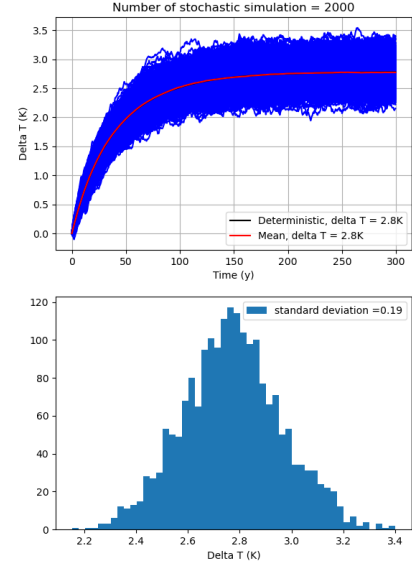


FIGURE 11 – Evolution of 2000 simulations following the stochastic equation eq. 14 with  $\lambda = -0.88Wm^{-2}K^{-1}$ ,  $\alpha = 0.058Wm^{-2}K^{-2}$  and  $\beta = -4 \times 10^{-8}Wm^{-2}K^{-5}$ . A forcing  $F = 2Wm^{-2}$  has been applied. The system is around deterministic steady state value after approximately 200 years, the standard deviation is  $0.19K$ .

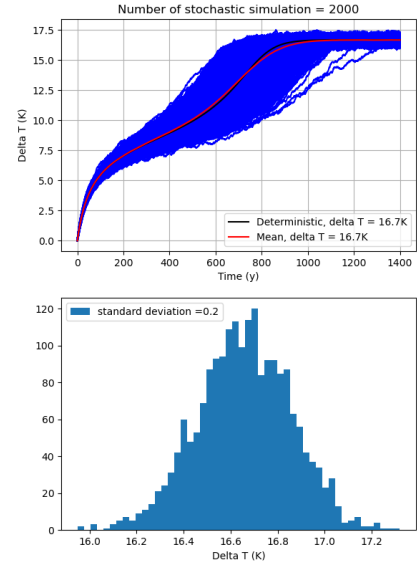


FIGURE 12 – Evolution of 2000 simulations following the stochastic equation eq. 14 with  $\lambda = -0.88Wm^{-2}K^{-1}$ ,  $\alpha = 0.058Wm^{-2}K^{-2}$  and  $\beta = -4 \times 10^{-8}Wm^{-2}K^{-5}$ . A forcing  $F = 3.7Wm^{-2}$  has been applied. The system is around deterministic steady state value after approximately 1100 years, the standard deviation is  $0.2K$ .

### On the tipping point

We want to see how the stochastic solution behaves just before the tipping point. We simulated 50 Stochastic evolution for  $F = 3.43 \text{ W m}^{-2}$  on fig. 15. We see that if the deterministic system stabilizes after  $\approx 1000y$  some stochastic solution pass through the equilibrium, pushed by there stochastic oscillations and find an other equilibrium at twice the precedent value. If we perform the simulation for a very long time we see that in the end all the stochastic simulations would tend to stabilize around the  $\Delta T \approx 16K$  equilibrium. We plotted on fig. 16 the evolution of the standard deviation and the mean value of fifty stochastic simulations with the same parameters, we note an increasing of standard deviation when the stochastic evolution pass from one equilibrium to an other. The maximum of standard deviation is reached when the mean value is at mid distance of the two equilibrium. At this moment there is the same number of scenarios at the two equilibrium points.

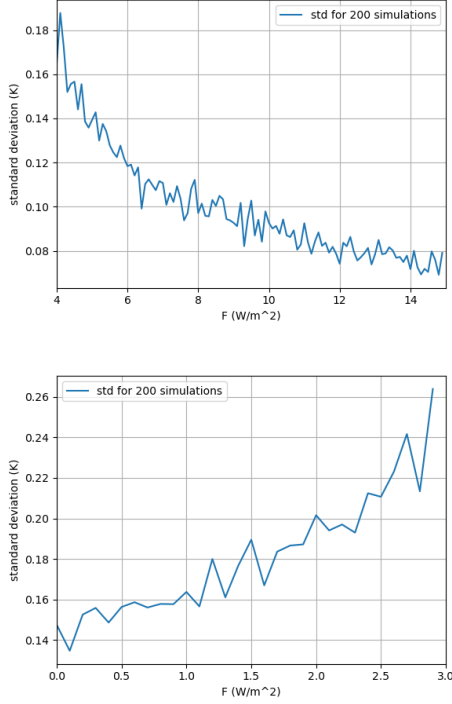


FIGURE 13 – Standard deviation of a set of 200 simulations at steady state. Parameters values were  $\lambda = -0.88 \text{ W m}^{-2} \text{ K}^{-1}$ ,  $\alpha = 0.058 \text{ W m}^{-2} \text{ K}^{-2}$  and  $\beta = -4 \times 10^{-8} \text{ W m}^{-2} \text{ K}^{-5}$ . **Above :** For a range of forcing from  $F = 4 \text{ W m}^{-2}$  to  $F = 15 \text{ W m}^{-2}$ . Std decreases when forcing increases. **Below :** For a range of forcing from  $F = 0 \text{ W m}^{-2}$  to  $F = 3 \text{ W m}^{-2}$ . Std increase with forcing.

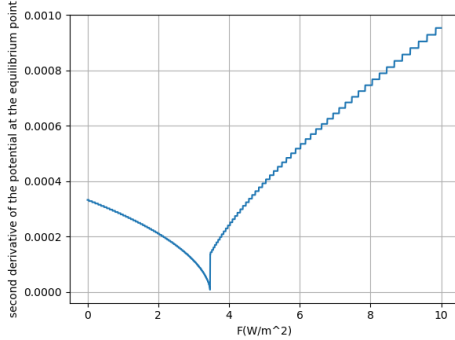


FIGURE 14 – Plot of the second derivative value of the potential function (in  $s^{-1}$ ) defined as eq. 13 at the equilibrium point with  $\lambda = -0.88 \text{ W m}^{-2} \text{ K}^{-1}$ ,  $\alpha = 0.058 \text{ W m}^{-2} \text{ K}^{-2}$  and  $\beta = -4 \times 10^{-8} \text{ W m}^{-2} \text{ K}^{-5}$ . We note that this value is always positive, i.e. the system always reach a stable equilibrium. There is a decrease before the tipping point and then an increase.

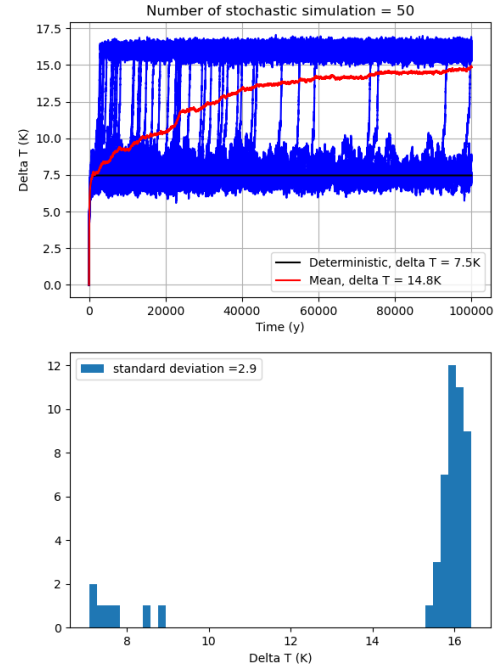


FIGURE 15 – Evolution of 50 simulations following the stochastic equation eq. 14 with  $\lambda = -0.88 \text{ W m}^{-2} \text{ K}^{-1}$ ,  $\alpha = 0.058 \text{ W m}^{-2} \text{ K}^{-2}$  and  $\beta = -4 \times 10^{-8} \text{ W m}^{-2} \text{ K}^{-5}$ . A forcing  $F = 3.43 \text{ W m}^{-2}$ , just before the tipping point, has been applied. We see that the deterministic solution has reached a steady state at  $\Delta T \approx 7.5K$  but the stochastic evolution tends to leave this path, being attracted by the  $\Delta T = 16K$  equilibrium.



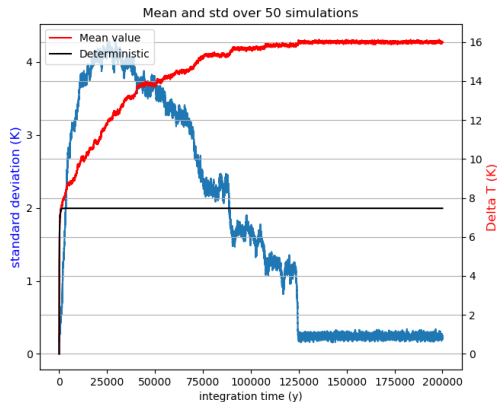


FIGURE 16 – *Standard deviation and mean value of 50 simulations following the stochastic equation eq. 14 with  $\lambda = -0.88Wm^{-2}K^{-1}$ ,  $\alpha = 0.058Wm^{-2}K^{-2}$  and  $\beta = -4 \times 10^{-8}Wm^{-2}K^{-5}$ . A forcing  $F = 3.43Wm^{-2}$ , just before the tipping point, has been applied.*

## CONCLUSION

We have investigated the quadratic dependence model in Part I. We have seen that the linear approximation holds valid at small scale - i.e. small integration time, small temperature variation or small forcing. However, the anthropogenic forcing perturbation that the earth system will face is in a range where the linear approximation won't be valid anymore. Indeed if we look at the four RCP scenarios used by the IPCC they are respectively concerning forcing of  $F = 2.6W/m^2$ ,  $F = 4.5W/m^2$ ,  $F = 6W/m^2$  and  $F = 8.5W/m^2$ . We have seen that, in these conditions, knowing the magnitude of the temperature feedback dependence is crucial. We have shown along the first part how little variation of  $\alpha$  could lead to several different behaviour of the planet sensitivity. For some parameter values, we have shown that the system could present a runaway warming and wasn't able to predict the warming  $\Delta T$  anymore.

To solve this problem we used a higher order equation. We saw that in the quadratic runaway warming cases, the system would reach a steady state far away from the first one. This changing of equilibrium state happens under a small change of forcing. While  $\Delta T$  increases gently with forcing below this point, its value doubles abruptly when it goes past it. We found that our system presented a tipping-point, a threshold above which the characteristic are changing suddenly.

It is important to note that if the higher order equation gives us a qualitative behaviour of the climate system after the tipping point, our ability to predict quantitatively the warming response depends on our knowledge about the  $\beta$

parameter. This kind of higher order parameter are really hard to estimate from present data because we have only access to a small range of temperature variation recorded in detail (this is detailed in "result" section of [1]).

We finally observed the system behaviour under chaotic fluctuations as the one observed in our current climate. We saw that the global behaviour of the stochastic evolution were following the deterministic evolution and the standard deviations were always largely inferior to the mean warming value. The only case where it was not true was just before the tipping point where stochastic evolution sometimes broke through the deterministic equilibrium point and passed to the quadratic runaway scenario. This behaviour highlights how the presence of tipping point increases the difficulty of predicting the system evolution. As this simple model suggest, tipping point in the earth sensitivity for a warming planet are possible. Knowing that, we should manage carefully our greenhouse gases emissions to avoid any dramatic runaway warming.

- 
- \* Electronic address: Augustin.Lambotte@student.uclouvain.be, Maxence.Malempre@student.uclouvain.be
- [1] Bloch-Johnson, J., R. T. Pierrehumbert, and D. S. Abbot (2015), Feedback temperature dependence determines the risk of high warming, *Geophys. Res. Lett.*, 42, 4973–4980, doi :10.1002/2015GL064240.
  - [2] Somerville, Richard C. J.; Remer, Lorraine A. (1984). Cloud optical thickness feedbacks in the CO2 climate problem. *Journal of Geophysical Research*, 89(D6), 9668–. doi :10.1029/jd089id06p09668
  - [3] Lunt, Daniel J.; Haywood, Alan M.; Schmidt, Gavin A.; Salzmann, Ulrich; Valdes, Paul J.; Dowsett, Harry J. (2009). Earth system sensitivity inferred from Pliocene modelling and data. , 3(1), 60–64. doi :10.1038/ngeo706
  - [4] Bloch-Johnson, J., Rugenstein, M., Stolpe, M. B., Rohrschneider, T., Zheng, Y., & Gregory, J. M. (2021). Climate sensitivity increases under higher CO2 levels due to feedback temperature dependence. *Geophysical Research Letters*, 48, e2020GL089074. <https://doi.org/10.1029/2020GL089074>
  - [5] Jonko, Alex & Shell, Karen & Sanderson, Benjamin & Danabasoglu, Gokhan. (2013). Climate Feedbacks in CCSM3 under Changing CO2Forcing. Part II : Variation of Climate Feedbacks and Sensitivity with Forcing. *Journal of Climate*. 26. 2784-2795. 10.1175/JCLI-D-12-00479.1.
  - [6] Timothy M. Lenton, Hermann Held, Elmar Krieger, Jim W. Hall, Wolfgang Lucht, Stefan Rahmstorf, and Hans Joachim Schellnhuber. (2007). Tipping elements in the Earth's climate system. Edited by William C. Clark, Harvard University, Cambridge, MA. <https://doi.org/10.1073/pnas.0705414105>
  - [7] Ashwin, P., von der Heydt, A.S. Extreme Sensitivity and Climate Tipping Points. *J Stat Phys* 179, 1531–1552 (2020). <https://doi.org/10.1007/s10955-019-02425-x>